Measurement of the ^{12}C(e,e′p)^{11}B Two-Body Breakup Reaction at High Missing Momentum Values

P. Monaghan[a], R. Shneor[b], R. Subedi[c], B. D. Anderson[c], K. Aniol[d], J. Annand[e], J. Arrington[f], H. Benaoum[g], F. Benmokhtar[h], P. Bertin[i], W. Bertozzi[a], W. Boeglin[j], J. P. Chen[k], Seonho Choi[l], E. Chudakov[k], C. Ciofi degli Atti[m], E. Cisbani[n], W. Cosyn[o], B. Craver[p], C. W. de Jager[k], R.J. Feuerbach[k], E. Folts[k], S. Frullani[q], F. Garibaldi[q], O. Gayou[a], S. Gilad[a], R. Gilman[r,k], O. Glamazdin[s], J. Gomez[k], O. Hansen[k], D. W. Higinbotham[k,*], T. Holmstrom[t], H. Ibrahim[u], R. Igarashi[v], E. Jans[w], X. Jiang[r], Y. Jiang[x], L. Kaufman[y], A. Kelleher[t], A. Kolarkar[z], E. Kuchina[r], G. Kumbartzki[r], J. J. LeRose[k], R. Lindgren[p], N. Liyanage[p], D. J. Margaziotis[d], P. Markowitz[j], S. Marrone[q], M. Mazouz[aa], D. Meekins[k], R. Michaels[k], B. Moffit[t,k], H. Morita[ab], S. Nanda[k], C. F. Perdrisat[t], E. Piasetzky[b], M. Potokar[ac], V. Punjabi[ae], Y. Qiang[a], J. Reinhold[j], B. Reitz[k], G. Ron[b], G. Rosner[e], J. Ryckebusch[o], A. Saha fn1][k,1], B. Sawatzky[p,af,k], J. Segal[k], A. Shahinyan[ag], S. Širca[ac,ad], K. Slifer[p,af], P. Solvignon[af,k], V. Sulkosky[t,a], N. Thompson[e], P. E. Ulmer[u], G. M. Urciuoli[q], E. Voutier[aa], K. Wang[p], J. W. Watson[c], L.B. Weinstein[u], B. Wojtsekhowski[k], S. Wood[k], H. Yao[af], X. Zheng[f,a], L. Zhu[ah]

[a]*Massachusetts Institute of Technology, Cambridge, Massachusetts 02139, USA*
[b]*Tel Aviv University, Tel Aviv 69978, Israel*
[c]*Kent State University, Kent, Ohio 44242, USA*
[d]*California State University Los Angeles, Los Angeles, California 90032, USA*
[e]*University of Glasgow, Glasgow G12 8QQ, Scotland, UK*
[f]*Argonne National Laboratory, Argonne, Illinois, 60439, USA*
[g]*Syracuse University, Syracuse, New York 13244, USA*
[h]*University of Maryland, College Park. Maryland 20742, USA*
[i]*Laboratoire de Physique Corpusculaire, F-63177 Aubière, France*
[j]*Florida International University, Miami, Florida 33199, USA*
[k]*Thomas Jefferson National Accelerator Facility, Newport News, Virginia 23606, USA*
[l]*Seoul National University, Seoul 151-747, Korea*
[m]*INFN, Sezione di Perugia , Via A. Pascoli I-06123, Perugia, Italy*
[n]*INFN, Sezione Sanitá and Istituto Superiore di Sanitá, Laboratorio di Fisica, I-00161 Rome, Italy*

[*]Corresponding Author
[1]Deceased

Preprint submitted to Elsevier *February 27, 2013*

[o] Ghent University, Proeftuinstraat 86, B-9000 Gent, Belgium
[p] University of Virginia, Charlottesville, Virginia 22904, USA
[q] INFN, Sezione Sanitá and Istituto Superiore di Sanitá, Laboratorio di Fisica, I-00161 Rome, Italy
[r] Rutgers, The State University of New Jersey, Piscataway, New Jersey 08855, USA
[s] Kharkov Institute of Physics and Technology, Kharkov 310108, Ukraine
[t] College of William and Mary, Williamsburg, Virginia 23187, USA
[u] Old Dominion University, Norfolk, Virginia 23508, USA
[v] University of Saskatchewan, Saskatoon, Saskatchewan, Canada S7N 5E2
[w] Nationaal Instituut voor Kernfysica en Hoge-Energiefysica, Amsterdam, The Netherlands
[x] University of Science and Technoogy of China, Hefei, Anhui, China
[y] University of Massachusetts Amherst, Amherst, Massachusetts 01003, USA
[z] University of Kentucky, Lexington, Kentucky 40506, USA
[aa] Laboratoire de Physique Subatomique et de Cosmologie, 38026 Grenoble, France
[ab] Sapporo Gakuin University, Bunkyo-dai 11, Ebetsu 069, Hokkaido, Japan
[ac] Institute "Jožef Stefan", 1000 Ljubljana, Slovenia
[ad] Dept. of Physics, University of Ljubljana, 1000 Ljubljana, Slovenia
[ae] Norfolk State University, Norfolk, Virginia 23504, USA
[af] Temple University, Philadelphia, Pennsylvania 19122, USA
[ag] Yerevan Physics Institute, Yerevan 375036, Armenia
[ah] University of Illinois at Urbana-Champaign, Urbana, Illinois 61801, USA

Abstract

The five-fold differential cross section for the $^{12}\mathrm{C}(e,e'p)^{11}\mathrm{B}$ reaction was determined over a missing momentum range of 200 – 400 MeV/c, in a kinematics regime with $x_B > 1$ and $Q^2 = 2.0$ (GeV/c)^2. A comparison of the results with theoretical models and previous lower missing momentum data is shown. The theoretical calculations agree well with the data up to a missing momentum value of 325 MeV/c and then diverge for larger missing momenta. The extracted distorted momentum distribution is shown to be consistent with previous data and extends the range of available data up to 400 MeV/c.

While the independent particle nuclear shell model has enjoyed much success in predicting properties of nuclei up to the Fermi momentum, upto approximately 250 MeV/c, the model breaks down at larger momenta [1]. Experiments at Saclay studying the $^{2}\mathrm{H}(e,e'p)n$ [2] and $^{3}\mathrm{He}(e,e'p)^{2}\mathrm{H}$ [3, 4] reactions showed that mean-field calculations provided good descriptions of

the data up to momenta of 250 MeV/c but highlighted the importance of final state interactions and mesonic degrees of freedom at higher momenta. These investigations were continued with experiments at NIKHEF and MIT-Bates, which studied the $(e, e'p)$ reaction for various nuclei from ^{2}H to ^{209}Bi [5, 6, 7, 8, 9]. The shape of the distorted momentum distributions were adequately described by calculations based on the distorted wave impulse approximation (DWIA) [10] up to the Fermi momentum. However, the observed spectroscopic strength, a multiplicitive factor required to match the predicted cross sections with data, for valence orbital knockout averaged around 0.65, significantly lower than predicted [11]. One explanation is that there are nucleon-nucleon correlations present, which were neglected in the calculations. The effect of such correlations would be to cause a depletion of valence states occupied below the Fermi momentum and an enhancement of continuum states occupied above the Fermi momentum. This translates into shifting strength from low missing momentum ($\vec{p}_m$, the momentum of the undetected residual system) and low missing energy (E_m, which accounts for the separation energy for removing a proton from the target nucleus and any excitation of the residual system) to higher missing momentum and energy in the A$(e, e'p)$ reaction. Previous experiments which studied inclusive [12, 13, 14, 15, 16], single nucleon knockout [17, 18, 19, 20] and multi-nucleon knockout reactions [17, 21, 22, 23, 24] have shown that kinematics with a large four-momentum transfer squared, $Q^2 = -q_\mu q^\mu = |\vec{q}^2| - \omega^2$ and Bjorken scaling variable, $x_B = Q^2/2m_p\omega > 1$, where ω and $\vec{q}$ are the energy and momentum transfer respectively from the initial electron during the interaction, are preferable for studying high p_m nucleon-nucleon correlations since these kinematics minimise competing effects such as meson-exchange currents (MEC), isobar configurations (IC) and final state interactions (FSI) [25, 26, 27, 28]. In this work, we examine the ^{12}C$(e, e'p)^{11}$B two-body breakup channel; the studies of short-range correlations related to this work from the ^{12}C$(e, e'pp)$ and ^{12}C$(e, e'pn)$ multi-nucleon knockout reaction channels have been published separately [29, 30].

The experiment was performed in Hall A at the Thomas Jefferson National Accelerator Facility (JLab), using the High Resolution Spectrometers (HRS) [31]. The data were taken at a fixed electron beam energy of 4.627 GeV incident on a 0.25 mm thick natural-carbon foil target. The scattered electrons were detected in the left HRS at a central scattering angle and momentum of 19.5° and 3.762 GeV/c, respectively. This fixed the electron kinematics, resulting in a central three-momentum transfer of $|\vec{q}| = 1.66$

GeV/c and energy transfer of $\omega = 0.865$ GeV, which corresponds to four momentum transfer squared of $Q^2 \simeq 2$ (GeV/c)^2 and Bjorken scaling variable, $x_B \simeq 1.23$. The knocked-out protons were detected in the right HRS with $|\vec{p}_p| = 1.45$ GeV/c and $\theta_p = 40.1°$ respectively. This spectrometer setting provided a continuous coverage of missing momentum from 200 to 400 MeV/c for the ^{12}C$(e, e'p)^{11}$B reaction where the missing momentum vector is defined as $\vec{p}_m = \vec{q} - \vec{p}_p$.

The peak in the missing energy distribution shown in Figure 1 results predominantly from knockout of protons from the $p_{3/2}$ shell, leaving the residual ^{11}B nucleus in its ground state. There is also a small contribution from proton knockout from other states, leaving the ^{11}B nucleus in a low-lying excited state. There is a large number of events at missing energies greater than 20 MeV resulting from knockout of protons from the s-shell in addition to knockout of protons from correlated nucleon–nucleon pairs. The histogram in red shows the results of a simulation normalized to the data that includes radiation of real photons by the electron (the 'radiative tail').

The $(e, e'p)$ events were selected by placing a 1.1 ns around the coincidence timing peak as well as using the HRS pion rejector to surpress the small amount of pion background. The resulting event sample, contained less then 1% randon events. The only other cuts on the data were the nominal HRS phase space cuts on momentum, $abs(dp/p) < 0.04\%$ and angular cuts of $abs(\theta) < 0.05$ radians and $abs(\phi) < 0.03$ radians about the spectrometers central ray.

A full simulation, including energy losses, multiple scattering, internal and external radiation and spectrometer resolutions was performed. The same set of acceptance cuts, which was applied to the data, was also applied to the simulation. The simulation program MCEEP (**M**onte **C**arlo for **e**, **e′ p**) [32] was used to extract the five-fold differential cross section from the data by using an iterative procedure to adjust the radiated ^{12}C$(e, e'p)$ cross section in the simulation until the simulated yield agreed with the experimental yield in each missing momentum bin.

The cross section model used in this analysis was based on the factorized distorted wave impulse approximation (DWIA) and is defined as [33],

$$\frac{d^6\sigma}{d\Omega_e d\Omega_p dE_e dE_p} = E_p \, p_p \, \sigma_{cc2} \, S_D(\vec{p}_m, E_m) \tag{1}$$

where σ_{cc2} is the single-nucleon off-shell cross section prescription of de Forest [33]. The σ_{cc2} prescription is a current-conserving off-shell extrapolation

of the on-shell current obtained from the Dirac equation. This prescription includes explicitly the four-momentum transfer (q^μ) in the nucleon current calculation, whereas the σ_{cc1} prescription does not; further details are given in [33]. $S_D(\vec{p}_m, E_m)$ is the proton part of the distorted spectral function and is the probability of finding a proton in the nucleus with momentum $\vec{p}_m$ and energy E_m.

The five-fold differential cross section for the bound state reaction is obtained by integrating the six-fold differential cross section over the missing energy of the two-body breakup peak. Integrating Eq. (1) over the missing energy peak in the discrete part of the ^{11}B spectrum leads to the five-fold differential cross section for a specfic state,

$$\frac{d^5\sigma}{d\Omega_e d\Omega_p dE_e} = K\sigma_{cc2} \int_{\Delta E_m} S_D\left(\vec{p}_m, E_{m'}\right) dE_{m'} \tag{2}$$

where $K = E_p p_p \eta^{-1}$ and η is the recoil factor required when integrating over the missing energy peak to arrive at the five-fold differential cross section given by

$$\eta = 1 - \frac{E_p}{E_r}\frac{\vec{p_p}\cdot\vec{p_r}}{|\vec{p_p}|^2} \tag{3}$$

and ΔE_m is the range of missing energy for the specific state being analyzed to account for the natural width of the final state along with the experimental energy resolution. In this analysis, a range of integration of 0 to 20 MeV was used to select events from the $p_{3/2}$-shell.

At sufficiently low values of the missing energy, the spectral function is centered around specific values of E_m and it can be assumed to factorize into two functions,

$$S_D\left(\vec{p}_m, E_m\right) = \sum_\alpha n_\alpha\left(\vec{p}_m\right) f_\alpha\left(E_m^\alpha\right) \tag{4}$$

where $f_\alpha\left(E_m^\alpha\right)$ is the missing energy distribution for state α and is sharply peaked about E_m^α and $n_\alpha\left(\vec{p}_m\right)$ is the missing momentum distribution for state α. The above considerations allow the cross section to be written as,

$$\frac{d^5\sigma}{d\Omega_e d\Omega_p dE_e} = K\sigma_{cc2}\, n_\alpha\left(\vec{p}_m\right) \int f_\alpha\left(E_m\right) dE_m. \tag{5}$$

Since the missing mass distribution function for a bound state is a delta function, the model cross section can be modified by adjusting the input momentum distribution $n_\alpha(\vec{p}_m)$ to the simulation.

An iteration procedure was used to fit the simulation yield to the experimental data. Starting with an initial input momentum function, the simulation was run and the resulting simulated yield as a function of missing momentum compared to the counts in the experimental data, with the same set of cuts being applied to both the simulation and the data. The difference between the simulated yield and the experimental data was used to then modify the input momentum function for the next simulation run. This iteration procedure continued until the simulated yield agreed with the experimental data; the value of the rational function $F(\vec{p}_m)$ at each missing momentum bin became approximately uniform with values ranging from 0.99 - 1.01. Thus, the experimental cross section is obtained by normalizing the factorized cross section model in the simulation to the data by,

$$\left\langle \frac{d^5\sigma}{d\Omega_e d\Omega_p dE_e} \right\rangle_{exp} = K\ \sigma_{cc2}\ f_n(\vec{p}_m) \prod_{i=1}^{i=n} F_i(\vec{p}_m) \tag{6}$$

where $f_n(\vec{p}_m)$ is the initial input momentum distribution after n iterations have been performed.

The dominate systematic error in this type of analysis turned out to be the exact placement of the limit on the E_M for selecting the $p_{3/2}$-shell and it was found that shifting the limit by ± 1 MeV, resulted in 5.9% variations in the resulting cross section. The next leading source of systematic error was the absolute normalized to elastic scattering which was determined to be 4.5%. Other minor sources of error included absolute tracking effeciency uncertainty of 1.1%, uncertainty on the radiative corrections of 1.0%; for a total systematic uncertainty of 7.6%.

The resulting five-fold differential cross section as a function of missing momentum is shown in Fig. 2. The first (inner) error bar on each data point is the statistical error; the second (outermost) error bar is the total error calculated from the sum in quadrature of the statistical error and the 7.6% systematic errors. The cross section data spans a range of missing momentum of 200 – 400 MeV/c. Although the electron spectrometer had a fixed momentum and angle setting throughout the experiment, the fact that both spectrometers have finite acceptances leads to each data point having slightly different values of Q^2 and ω for the missing momentum value of that bin. Also shown in Fig. 2 are four curves produced by calculations utilising different models. Each calculation has been performed using the appropriate kinematics for each missing momentum bin, rather than only the central spectrometer setting.

The RMSGA and RMSGA + FSI_{SRC} curves in Fig. 2 are calculations using unfactorized relativistic formulations of Glauber multiple scattering theory [34] by W. Cosyn and J. Ryckebusch. The bound-state wave functions are solutions to the Dirac equation with scalar and vector potentials fitted to ground-state nuclear properties. The final state interactions do not use optical potentials but instead are modelled on rescattering of a fast proton from a composite target containing $A - 1$ *frozen* spectator nucleons. The curve labelled 'RMSGA+FSI_{SRC}' differs from the 'RMSGA' calculation in that it has been extended to include short-range correlation effects in the final state interactions [35]. These correlations create local fluctuations in the nuclear density, changing the attenuation of the scattered proton in the nuclear medium.

The WS + Glauber curve in Fig. 2 corresponds to a factorized calculation by C. Ciofi degli Atti and H. Morita [36]. This model uses a Woods-Saxon form for the proton wave function. The final state interactions are modeled using an improved Glauber approach [37] to describe the rescattering of the struck proton [38, 39, 40]. This calculation includes ground state correlations in the initial wave function which result in a reduction of the cross section by a factor of 0.8. This has the effect of reducing the occupation number of the $1p_{3/2}$ shell predicted by an independent particle shell model.

The PWIA curve corresponds to a Plane Wave Impulse Approximation calculation. This curve does not agree with the data and demonstrates the importance of including final state interactions in a fully relativistic framework for theoretical calculations of this reaction. At missing momentum values larger than 300 MeV/c, other factors such as correlations in the ground state and final state wavefunctions modify the behaviour of the calculations further.

The experimental distorted momentum distribution can then be extracted from the cross section data by dividing out the kinematic factor and the single nucleon off-shell cross section from Eq. 6. This was accomplished by running another MCEEP simulation, with all of the input parameters unchanged, except now with a uniform input momentum function. This meant that all of the same averaging over the same missing momentum bins as was done for the cross section extraction was repeated for this simulation to generate just the kinematic factor and the single nucleon off-shell cross section. The

distorted momentum distribution is then given by,

$$n_{distorted}(p_m) = \left\langle \frac{d^5\sigma}{d\Omega_e d\Omega_p dE_e} \right\rangle_{exp} / \left\langle K\sigma_{cc2} \right\rangle_{unit} \tag{7}$$

The experimental distorted momentum distribution from this experiment covers a range in missing momentum of -200 to -400 MeV/c, which overlaps with data from a previous experiment in Hall C at JLab [41]. A comparison of the experimental distorted momentum distributions from both experiments along with calculated momentum distributions arising from the models used to calculate the cross sections in Fig. 2 are shown in Fig. 3. The data from the Hall C experiment shown here was taken at $Q^2 = 1.8$ (GeV/c)^2, and includes a cut on missing energy of $15 < E_m < 25$ MeV to select the p-shell; however, this missing energy range does include some contribution from s-shell knockout. The Hall C analysis includes a factor of $(2j + 1)$ for the multiplicity of the shell being considered. This analysis extracted the cross section per nucleon and so to make this comparison, our data are multiplied by a factor of 4.

As Fig. 3 shows, the two experiments agree in the overlap momentum region from -200 to -300 MeV/c. The data from this experiment extends the experimental momentum distribution to -400 MeV/c. The resulting momentum distributions from the PWIA, RMSGA and WS+Glauber calculations are compared to the data in Fig. 3. The RMSGA and WS+Glauber calculations are in good agreement with the data from both experiments and each other up to a missing momentum around 325 MeV/c, where they start to diverge slightly. At higher missing momentum, the differences between the calculations, can be traced to different treatments of correlations in the initial and final state wavefunctions.

For completeness, the experimental cross section and extracted momentum distribution results are shown in Table 1. The statistical and systematic uncertainties for each data point are quoted separately. The systematic uncertainty includes normalisation, kinematic and event selection uncertainties, all added together in quadrature to produce a single value. The average values of Q^2 and ω as well as their RMS widths for each missing momentum bin are also provided.

In summary, the experimental five-fold differential cross section for the ^{12}C$(e, e'p)^{11}$B reaction has been extracted in a previously unexplored kinematic region. The data extends over a range of missing momenta from 200 – 430 MeV/c. A comparison of PWIA and fully relativistic calculations which

p_m [MeV/c]	$\frac{d^5\sigma}{d\Omega_e d\Omega_p dE_e} \pm \delta_{stat}$ [fm^2/(MeV-sr^2)]	$n(p_m)$ [MeV^{-3}]	$\bar{Q}^2 \pm \sigma_{Q^2}$ [(GeV/c)^2]	$\bar{\omega} \pm \sigma_\omega$ [MeV]
190	2.62e-08 ± 13.5%	2.29e-08	1.70 ± 0.018	852 ± 4.2
210	2.18e-08 ± 6.3%	2.03e-08	1.72 ± 0.033	846 ± 8.4
230	1.09e-08 ± 5.3%	1.09e-08	1.74 ± 0.046	841 ± 12.5
250	4.95e-09 ± 5.4%	5.31e-09	1.77 ± 0.060	836 ± 16.6
270	2.47e-09 ± 5.7%	2.85e-09	1.80 ± 0.075	830 ± 20.7
290	1.13e-09 ± 7.0%	1.42e-09	1.83 ± 0.088	824 ± 23.9
310	6.20e-10 ± 8.3%	8.48e-10	1.87 ± 0.103	819 ± 26.0
330	3.73e-10 ± 10.2%	5.66e-10	1.92 ± 0.117	815 ± 27.1
350	1.60e-10 ± 14.5%	2.76e-10	1.98 ± 0.128	814 ± 27.8
370	7.56e-11 ± 21.2%	1.50e-10	2.05 ± 0.134	813 ± 28.0
390	4.77e-11 ± 29.3%	1.09e-10	2.11 ± 0.130	813 ± 27.7

Table 1: Results for the ^{12}C(e,e$'$p)^{11}B reaction data from the highest proton momentum spectrometer setting. For each missing momentum bin, the average values of Q^2 and ω and their corresponding RMS widths σ_{Q^2} and σ_ω are given. Not shown is the global systematic error of 7.6%.

include final state interactions clearly demonstrates the failure of PWIA to describe the data. Indeed it highlights the need for theoretical calculations to include final state interactions within a fully relativistic framework, to obtain the correct magnitude of the cross section. The experimental data shows an inflection point around 325 MeV/c, when it stops decreasing exponentially. This is likely due to nucleon-nucleon correlations. The fact that the full theoretical calculations follow this trend as well shows the importance of including correlations in either the ground state or final state wavefunctions. The variations between the calculations at larger missing momenta above 325 MeV/c shows the effect of the different ingredients used in each calculation.

The experimental distorted momentum distribution was also extracted from the cross section data and compared with a previous experiment in Hall C at JLab. The data from both experiments are consistent for the region of missing momentum where they overlap. The theoretical calculations also showed good agreement with the data up to a missing momentum around 325 MeV/c, when they started to diverge slightly. The data from this experiment extends the missing momentum range of the distorted momentum

distribution, $n_D(\vec{p}_m)$, over which theorists can compare their calculations and improve their models.

We would like to acknowledge the contribution of the Hall A collaboration, the Hall A technical staff and the accelerator operations staff. This work was supported by the Israel Science Foundation, the US-Israeli Bi-national Scientific Foundation, the UK Engineering and Physical Sciences Research Council, the U.S. National Science Foundation, the U.S. Department of Energy grants DE-FG02-94ER40844, DE-AC02-06CH11357, DE-FG02-94ER40818, contract number DE-FG02-94ER40818 and U.S. DOE Contract No. DE-AC05-84150, Modification No. M175, under which the Southeastern Universities Research Association, Inc. operates the Thomas Jefferson National Accelerator Facility.

References

[1] J. J. Kelly, Adv. Nucl. Phys. 23 (1996) 75.

[2] S. Turck-Chieze et al., Phys. Lett. 142B (1984) 145.

[3] P. H. M. Keizer et al., Phys. Lett. 157B (1985) 255.

[4] C. Marchand et al., Phys. Rev. Lett. 60 (1988) 1703.

[5] P. K. A. de Witt Huberts, J. Phys. G16 (1990) 507.

[6] G. Van Der Steenhoven et al., Nucl. Phys. A480 (1988) 547. doi:10.1016/0375-9474(88)90463-0.

[7] K. I. Blomqvist et al., Phys. Lett. B344 (1995) 85. doi:10.1016/0370-2693(94)01540-S.

[8] P. E. Ulmer et al., Phys. Rev. Lett. 59 (1987) 2259. doi:10.1103/PhysRevLett.59.2259.

[9] L. B. Weinstein et al., Phys. Rev. Lett. 64 (1990) 1646. doi:10.1103/PhysRevLett.64.1646.

[10] S. Boffi, C. Giusti and F. D. Pacati, Phys. Rept. 226 (1993) 1. doi:10.1016/0370-1573(93)90132-W.

[11] L. Lapikas, Nucl. Phys. A553 (1993) 297–308.

[12] L. Frankfurt, M. Strikman, D. Day and M. Sargsian, Phys.Rev. C48 (1993) 2451. doi:10.1103/PhysRevC.48.2451.

[13] J. Arrington et al., Phys. Rev. Lett. 82 (1999) 2056. doi:10.1103/PhysRevLett.82.2056.

[14] K. S. Egiyan et al., Phys. Rev. C68 (2003) 014313.

[15] K. S. Egiyan et al., Phys. Rev. Lett. 96 (2006) 082501.

[16] N. Fomin et al., Phys.Rev.Lett. 108 (2012) 092502. doi:10.1103/PhysRevLett.108.092502.

[17] L. J. H. M. Kester et al., Phys. Rev. Lett. 74 (1995) 1712. doi:10.1103/PhysRevLett.74.1712.

[18] D. Rohe et al., Phys.Rev.Lett. 93 (2004) 182501. doi:10.1103/PhysRevLett.93.182501.

[19] W. Boeglin et al., Phys.Rev.Lett. 107 (2011) 262501. doi:10.1103/PhysRevLett.107.262501.

[20] J. Arrington, D. Higinbotham, G. Rosner and M. Sargsian, Prog. Part. Nucl. Phys. 67 (2012) 898. doi:10.1016/j.ppnp.2012.04.002.

[21] B. Zhang, Ph.D. thesis, Massachusetts Institute of Technology (2003).

[22] R. A. Niyazov et al., Phys. Rev. Lett. 92 (2004) 052303. doi:10.1103/PhysRevLett.92.052303.

[23] A. Tang et al., Phys. Rev. Lett. 90 (2003) 042301.

[24] E. Piasetzky, M. Sargsian, L. Frankfurt, M. Strikman and J. W. Watson, Phys. Rev. Lett. 97 (2006) 162504. doi:10.1103/PhysRevLett.97.162504.

[25] L. L. Frankfurt, M. M. Sargsian and M. I. Strikman, Phys. Rev. C56 (1997) 1124.

[26] R. G. Arnold et al., Phys. Rev. C 42 (1) (1990) R1–R5. doi:10.1103/PhysRevC.42.R1.

[27] J. M. Laget, Phys. Lett. B199 (1987) 493. doi:10.1016/0370-2693(87)91615-7.

[28] J. Ryckebusch, D. Debruyne, W. Van Nespen and S. Janssen, Phys. Rev. C60 (1999) 034604. doi:10.1103/PhysRevC.60.034604.

[29] R. Shneor et al., Phys. Rev. Lett. 99 (2007) 072501. doi:10.1103/PhysRevLett.99.072501.

[30] R. Subedi et al., Science 320 (2008) 1476. doi:10.1126/science.1156675.

[31] J. Alcorn et al., Nucl. Instrum. Meth. A522 (2004) 294.

[32] P. Ulmer, et al., MCEEP: Monte Carlo for (e,e'p) Experiments, hallaweb.jlab.org/software/mceep/mceep.html.

[33] T. De Forest, Nucl. Phys. A392 (1983) 232.

[34] J. Ryckebusch et al., Nucl. Phys. A 728 (2003) 226. doi:10.1016/j.nuclphysa.2003.08.022.

[35] W. Cosyn, M. C. Martínez and J. Ryckebusch, Phys. Rev. C 77 (2008) 034602. doi:10.1103/PhysRevC.77.034602.

[36] C. Ciofi degli Atti, H. Morita, M. Alvioli, To be Published.

[37] R. J. Glauber, Lectures in Theoretical Physics, Interscience Publishers, Inc., New York, 1959.

[38] H. Morita, C. Ciofi degli Atti and D. Treleani, Phys.Rev. C60 (1999) 034603. doi:10.1103/PhysRevC.60.034603.

[39] C. Ciofi degli Atti, L. Kaptari and H. Morita, Nucl. Phys. A782 (2007) 191. doi:10.1016/j.nuclphysa.2006.10.010.

[40] C. Ciofi delgi Atti and L. Kaptari, Phys. Rev. Lett. 100 (2008) 122301. doi:10.1103/PhysRevLett.100.122301.

[41] D. Dutta et al., Phys. Rev. C 68 (6) (2003) 064603. doi:10.1103/PhysRevC.68.064603.

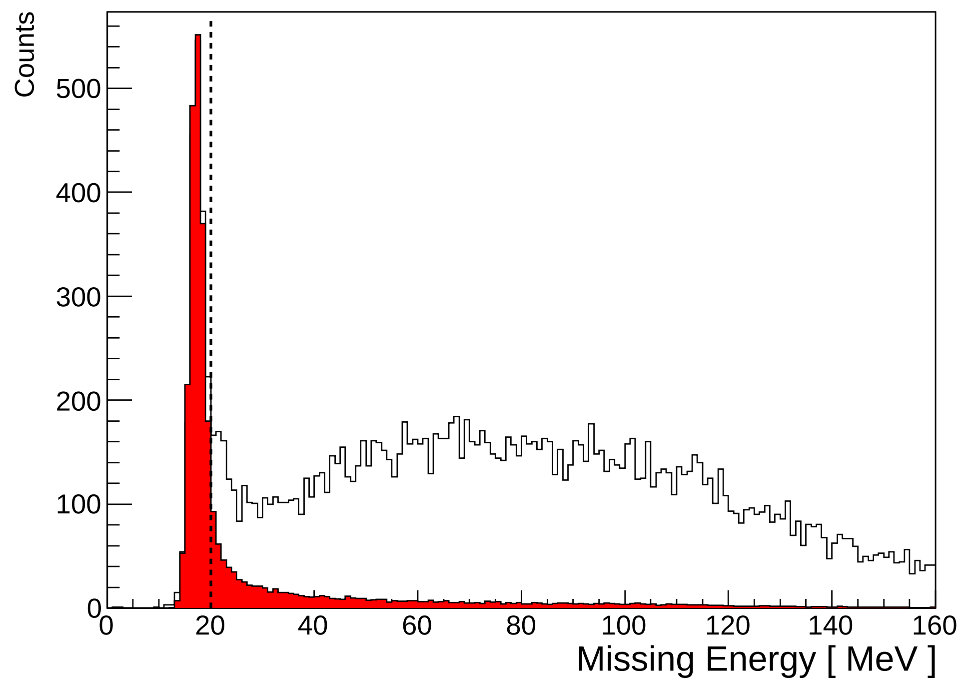

Figure 1: Number of counts versus missing energy for the proton spectrometer central momentum of 1.45 GeV/c. The peak around 16 MeV corresponds to proton knockout from the lowest states of carbon, predominantly the $p_{3/2}$ state. The filled region indicates the simulated data set used for this analysis of the $p_{3/2}$-shell knockout. The filled histogram (simulated events) also shows the tail of events extending out to large missing energy values, which result from real photons radiated out by the electron. The dotted vertical line shows the cut at 20 MeV used on the experimental data to separate out the events from the $p_{3/2}$-shell.

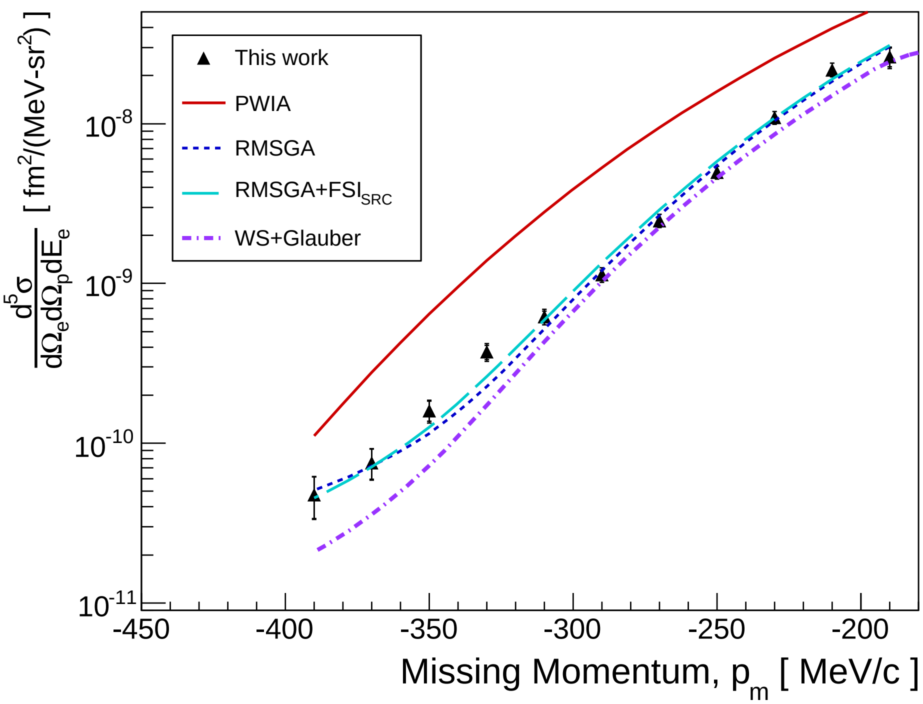

Figure 2: Experimental five-fold differential cross section extracted from the data are compared to several different theoretical calculations. In each theoretical calculation, full occupancy of the $1p_{3/2}$ shell has been assumed and no spectroscopic factor has been applied. Each data point is plotted at the center of a 20 MeV wide missing momentum bin. The difference between the PWIA calculation and the others demonstrates the importance of properly including effects such as correlations and final-state interactions to discribe the experimental results.

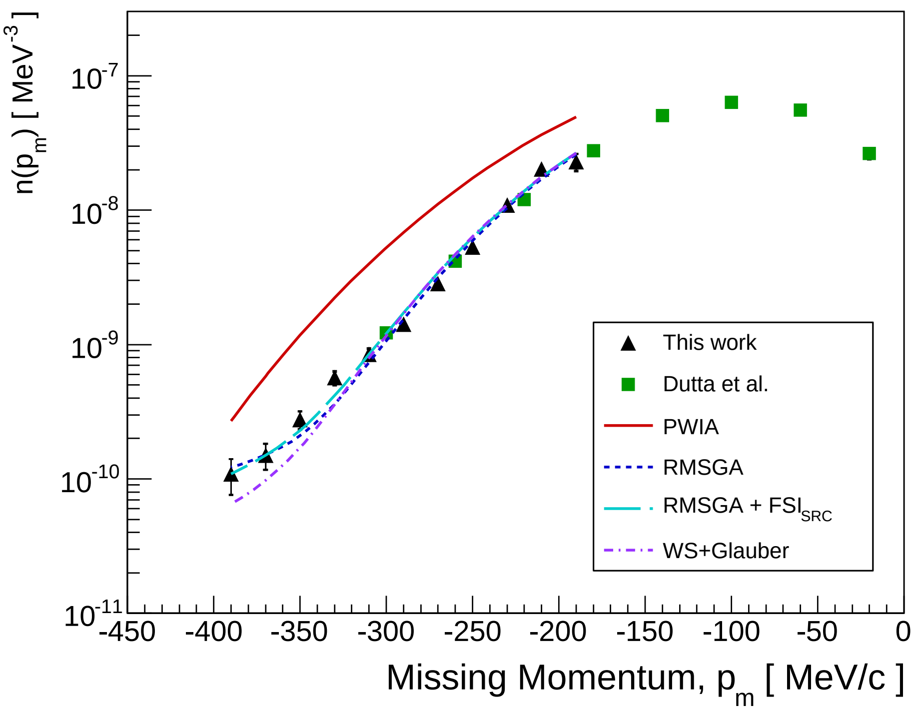

Figure 3: Comparison of experimental distorted momentum distribution extracted from two different experiments with theoretical calculations based on the RMSGA and WS+Glauber approaches, as well as a simple PWIA calculation. The agreement with the experimental data shows the same general trends as observed in the cross section comparison that correlations and final-state interations are required ingrediatants to discribe the data.